benzoyl ester **2** with use of this procedure was 38%.

A number of alternative procedures were investigated. The reaction of the nickel(II) macrocycle **1** with benzoyl chloride in dry chloroform and with triethylamine and catalytic 4-(dimethylamino)pyridine gave only a 13% yield of the benzoyl ester **2**. Use of benzene as the reaction solvent failed to give improved yields, although the procedure served to dry the nickel(II) complex. However, alternative procedures showed that a stoichiometric amount of 4-(dimethylamino)pyridine does indeed give results superior to those obtained with comparable amounts of triethylamine or those with catalytic amounts of 4-(dimethylamino)pyridine. In the optimized procedures, acetylations were performed in either dry chloroform or dry dichloromethane under a nitrogen atmosphere with a suspension of the macrocyclic nickel(II) complex **1**.

An infrared spectrum of the acetylation product showed a carbonyl band at 1735 cm^{-1}, which was not present in the infrared spectrum of the starting material. The spectrum also showed complete loss of the hydroxyl OH stretching frequency. The ^{13}C NMR spectrum of the product dissolved in deuterochloroform indicated 11 carbon environments and is fully consistent with structure **3**. The proton NMR spectrum was also examined at an operating frequency of 200 MHz. The protons of the saturated six-membered chelate ring are of particular interest. Those in the pair of methylene groups give rise to an AB quartet of doublets centered at 3.66 ppm. The AB quartet corresponds to a geminal coupling of $^2J_{HH}$ = 13.6 Hz between protons resonating at 3.76 and 3.58 ppm. The further coupling of these protons is due to the proton on the mirror plane of the complex with $^3J_{HH}$ = 5.7 Hz. This proton itself appears as a quintet at 4.82 ppm. All other resonances in the ^1H NMR spectrum appear as singlets.

The acetylation of the macrocyclic nickel(II) complex **1** was also attempted in dry dichloromethane with use of acetic acid and the coupling reagent *N,N'*-dicyclohexylcarbodiimide. No evidence of acetylation was found with infrared spectroscopy, and most of the starting material was recovered.

Conclusions

The acylation of noncoordinated hydroxyl groups in transition-metal complexes can be achieved under mild conditions. We believe that earlier reports concerning the low reactivity of hydroxyl groups in transition-metal complexes was due to ill-defined coordination environments, inappropriate reaction conditions, or the charged nature of the complexes.

Acknowledgment. The financial support of the U.S. National Institutes of Health (Grant No. GM10040) and the U.S. National Science Foundation (Grant No. CHE-8402153) is greatly appreciated.

Contribution from the Department of Chemistry and Biochemistry, University of Colorado, Boulder, Colorado 80309

Charge Distribution in Transition-Metal Complexes of a Schiff Base Biquinone Ligand. Structural and Electrochemical Properties of the M^{II}(Cat-N-BQ)$_2$, M^{III}(Cat-N-BQ)(Cat-N-SQ), M^{IV}(Cat-N-SQ)$_2$ Tautomeric Series

Cathy L. Simpson, Steven R. Boone, and Cortlandt G. Pierpont*

Received January 11, 1989

Reactions carried out between 3,5-di-*tert*-butylsemiquinone and ammonia in the presence of a divalent metal ion yield bis complexes of the resulting Schiff base biquinone ligand. The free ligand may chelate with metal ions in forms ranging in charge from 0 to −3, related by successive reduction steps of the two quinone units of the ligand. Three common electronic forms have been found to exist for complexes of these ligands, with the forms related by intramolecular transfer of charge between localized ligand and metal electronic levels. If the metal ion used in the synthetic procedure is redox inactive, the M^{II}(Cat-N-BQ)$_2$ form of the complex is obtained. With divalent metal ions that are subject to oxidation the M^{III}(Cat-N-BQ)(Cat-N-SQ) or M^{IV}(Cat-N-SQ)$_2$ form may result. In this report characterization of the bis(biquinonato)iron complex is presented, which indicates that the metal is high-spin ferric iron and that the complex exists in the mixed-charge ligand form Fe^{III}(Cat-N-BQ)(Cat-N-SQ). The complex has an $S = 2$ magnetic ground state, normally associated with high-spin ferrous complexes, due to spin coupling between the radical Cat-N-SQ^{2-} ligand and the metal. This complex and the nickel complex Ni^{II}(Cat-N-BQ)$_2$, which differs in charge distribution, have been characterized structurally. Both crystallize in the triclinic space group $P\bar{1}$, with $Z = 2$, in unit cells of the following dimensions: Fe($C_{28}H_{40}NO_2$)$_2$, a = 11.753 (3) Å, b = 12.286 (3) Å, c = 20.811 (6) Å, α = 83.26 (2)°, β = 73.62 (2)°, γ = 75.54 (2)°; Ni($C_{28}H_{40}NO_2$)$_2$, a = 11.703 (2) Å, b = 12.377 (3) Å, c = 20.703 (4) Å, α = 89.05 (2)°, β = 73.78 (2)°, γ = 75.48 (2)°. Structural features of the ligands, with results obtained earlier on the Co and Mn complexes, have been used to show how a consistent pattern of C–O, C–N, and ring C–C bond lengths provides information on ligand charge and on charge distribution within the complex. Examples of complexes in the three charge distribution forms have been studied by using cyclic voltammetry to identify characteristic differences in electrochemistry. Surprisingly, all three types undergo similar electrochemical processes. They show two reversible or quasireversible oxidations, two reversible or quasireversible reductions, and, in some cases, a third irreversible reduction. Charge assignments for the products of the redox processes demonstrate coordination of the biquinone ligand in forms ranging in charge from the neutral radical SQ-N-BQ to the Cat-N-Cat^{3-} trianion.

Introduction

Questions concerning charge distribution between ligand and metal have contributed to the interest in complexes of the semiquinonate and catecholate ligands.[1] This results from a similarity in energy between metal and quinone electronic levels, and similar questions exist for the complexes of polyquinone ligands. Complexes of a Schiff base biquinone ligand prepared by condensation of 3,5-di-*tert*-butyl-1,2-semiquinone with ammonia have been investigated.[2,3] The ligand (**1**) may coordinate with metal ions in forms ranging in charge from 0 to −3. A +1 diimine form may also exist, but its interaction with metals may differ from the neutral and anionic forms. In the absence of a metal ion with readily available coordination sites, cyclization occurs to give the phenoxazinylate radical anion (**2**).[4] Studies carried out on

(1) Pierpont, C. G.; Larsen, S. K.; Boone, S. R. *Pure Appl. Chem.* **1988**, *60*, 1331.

(2) Girgis, A. Y.; Balch, A. L. *Inorg. Chem.* **1975**, *14*, 2724.

(3) Larsen, S. K.; Pierpont, C. G. *J. Am. Chem. Soc.* **1988**, *110*, 1827.

(4) deLearie, L. A.; Haltiwanger, R. C.; Pierpont, C. G. *Inorg. Chem.* **1989**, *28*, 644.

0020-1669/89/1328-4379$01.50/0

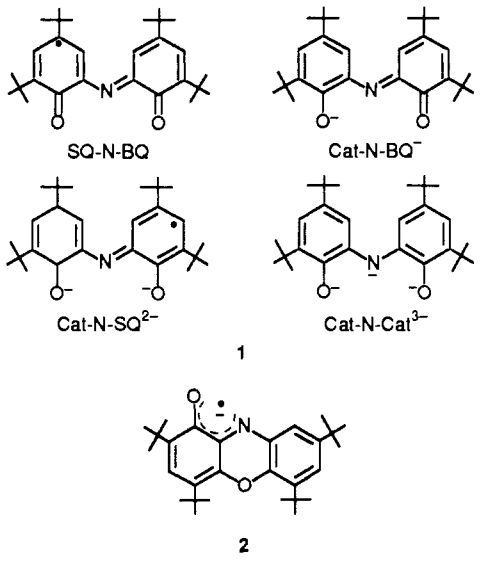

1

2

complexes of the biquinone ligand have shown that it may coordinate in either the monoanionic Cat-N-BQ$^-$ form or as the Cat-N-SQ^{2-} radical dianion.[3] Extensive charge delocalization might be expected for the ligand and for the resulting complexes. However, the mixed-ligand Co(III) complex Co(Cat-N-BQ)(Cat-N-SQ), which contains one unpaired electron associated with the radical ligand, showed coupling to the metal and to only one ring proton in its EPR spectrum. This suggested a surprisingly localized electronic structure with spin density concentrated in a single region of one ligand.[3] While the structural features of this complex failed to show an electronic difference between ligands, C–O, C–N, and ring C–C lengths might be sensitive to ligand charge. Bond length criteria that are similar to those developed for the benzoquinone, semiquinonate, and catecholate complexes[5] may provide insights into charge distribution in the biquinone complexes. We now report structural characterization on a bis(biquinone) complex of a metal that is clearly divalent for comparison with the structures of the neutral Co(III) and Mn(IV) complexes. We also provide characterization on the neutral bis(biquinonato)iron complex, which could contain either Fe(II) or Fe(III). Redox activity may be expected for the ligand and, possibly also, the metal ion of the bis(biquinone) complex. The electrochemical properties of the three types of complexes, M^{II}(Cat-N-SQ)$_2$, M^{III}(Cat-N-BQ)(Cat-N-SQ), and M^{IV}(Cat-N-SQ)$_2$, may further reflect charge distribution. To examine this possibility, the electrochemistry of complexes from all three classes has been studied.

Experimental Section

Synthetic Procedures. All complexes were prepared by using procedures described earlier.[2,3] In a typical reaction 1.06 g (4.8 mmol) of 3,5-di-*tert*-butylcatechol dissolved in 60 mL of 95% ethanol was added to a solution containing 1.0 mmol of the hydrated salt of the divalent metal ion dissolved in 10 mL of water. Concentrated aqueous ammonia, 5.0 mL, was added to the solution, the mixture was stirred in air for several hours, and the solid product was separated from the solution by filtration. Yields were typically in the 70%–80% range. Crystals satisfactory for X-ray analysis were grown by slow evaporation of dichloromethane/ethanol solutions of the complexes.

Physical Measurements. Infrared spectra were recorded on an IBM IR/30 FTIR spectrometer with samples prepared as KBr pellets. UV–vis spectra were recorded on a Hewlett Packard 8451A diode array spectrophotometer. Magnetic susceptibility measurements were made by the Faraday technique at room temperature. The Mössbauer spectrum of the iron complex was obtained in collaboration with Professor David Hendrickson of the University of Illinois. Cyclic voltammograms were obtained by using a BAS-100 electrochemical analyzer. A platinum-disk working electrode and a platinum-wire counter electrode were used. Tetra-*n*-butylammonium hexafluorophosphate was used as the supporting electrolyte, and the ferrocene/ferrocenium couple was used as an internal standard.

(5) Pierpont, C. G.; Buchanan, R. M. *Coord. Chem. Rev.* **1981**, *38*, 45.

Table I. Crystal Data for Ni(Cat-N-BQ)$_2$ and Fe(Cat-N-BQ)(Cat-N-SQ)

	Ni-(Cat-N-BQ)$_2$	Fe-(Cat-N-BQ)-(Cat-N-SQ)
formula	$NiC_{56}H_{80}N_2O_4$	$FeC_{56}H_{80}N_2O_4$
mol wt	903.90	901.05
space group	$P\bar{1}$	$P\bar{1}$
a, Å[b]	11.703 (2)	11.753 (3)
b, Å	12.377 (3)	12.286 (3)
c, Å	20.703 (4)	20.811 (6)
α, deg	89.05 (2)	83.26 (2)
β, deg	73.78 (2)	73.62 (2)
γ, deg	75.48 (2)	75.54 (2)
V, Å^3	2783 (1)	2788 (1)
Z	2	2
T, K	294–297	
λ, Å	0.71073 (Mo Kα)	
ρ_{meas}, g/cm^3[c]	1.08 (2)	1.08 (2)
ρ_{calc}, g/cm^3	1.08	1.07
μ, cm^{-1}	3.9	3.2
R, R_w[d] (obsd data)	0.052, 0.069	0.043, 0.062

[a] *International Tables for X-ray Crystallography*; Kynoch Press: Birmingham, England, 1965; Vol. 1. [b] Cell dimensions were determined by least-squares fit of the setting angles for 25 reflections with 2θ in the range 33–42° for Fe(Cat-N-BQ)(Cat-N-SQ) and 17–35° for Ni(Cat-N-BQ)$_2$. [c] By flotation methods in $ZnBr_2$ solution. [d] The quantity minimized in the least-squares procedure is $\sum w(|F_o| - |F_c|)^2$. $R = \sum||F_o| - |F_c||/\sum|F_o|$; $R_w = [\sum w(|F_o| - |F_c|)^2/\sum w(F_o)^2]^{1/2}$.

Crystallographic Structure Determinations on Fe($C_{28}H_{40}NO_2$)$_2$ and Ni($C_{28}H_{40}NO_2$)$_2$. Crystals of both complexes were mounted on glass fibers and aligned on a Nicolet P3/F automated diffractometer. Photographs taken on the crystals indicated triclinic symmetry and indicated that the complex molecules were approximately isostructural. Crystallographic data are given in Table I, and details of the structure determination and refinement are contained in a table included with the supplementary material. Final positional and isotropic thermal parameters for the two structure determinations are given in Tables II and III. Additional tables containing anisotropic thermal parameters and structure factors are available as supplementary material.

Experimental Results

The tridentate ligand formed by condensation of 3,5-di-*tert*-butylsemiquinone and ammonia may exist in electronic forms ranging in charge from +1 to −3 (**1**). However, only the monoanionic Cat-N-BQ$^-$ and dianionic radical Cat-N-SQ^{2-} forms have been observed to contribute significantly to the coordination chemistry of the ligand.[2,3] In the absence of available coordination sites on a metal ion, the ligand cyclizes to give the phenoxyazinylate radical anion (**2**).[4] When the reaction is carried out in the presence of a labile divalent metal ion, chelation occurs to give a neutral complex product with two biquinone ligands per metal ion. Options for charge distribution within the complex include M^{II}(Cat-N-BQ)$_2$, M^{III}(Cat-N-BQ)(Cat-N-SQ), and M^{IV}(Cat-N-SQ)$_2$ related by internal transfer of charge between ligand and metal. Complexes of all three forms have been characterized. In cases where the metal ion is not readily subject to oxidation the M^{II}(Cat-N-BQ)$_2$ charge distribution is found. Girgis and Balch reported examples of complexes in this form with Ni, Cu, Zn, Cd, and Mg.[2] Reactions carried out with Co^{2+} and Mn^{2+} gave Co^{III}(Cat-N-BQ)(Cat-N-SQ) and Mn^{IV}(Cat-N-SQ)$_2$ by internal transfer of charge to the ligands.[3]

The neutral iron complex,[2] prepared by using the procedure described above beginning with Fe^{2+}, could contain either ferrous or ferric iron. The product of this reaction has been examined by using Mössbauer spectroscopy. At 100 K the complex showed a single quadrupole-split doublet with an isomer shift value of 0.4164 (5) mm/s (vs iron foil) and a quadrupole splitting parameter of 0.4794 (10) mm/s. These values are quite typical of high-spin Fe(III),[6] and the charge distribution for the complex

(6) Boone, S. R.; Purser, G. H.; Chang, H.-R.; Lowery, M. D.; Hendrickson, D. N.; Pierpont, C. G. *J. Am. Chem. Soc.* **1989**, *111*, 2292.

Table II. Atomic Coordinates ($\times 10^4$) and Equivalent Isotropic Displacement Parameters ($Å^2 \times 10^3$) for $Fe(C_{28}H_{40}NO_2)_2$

atom	x/a	y/b	z/c	U[a]
Fe	2343 (1)	2704 (1)	2486 (1)	42 (1)
N1	3419 (2)	2630 (2)	1486 (1)	37 (1)
N2	1328 (2)	2625 (2)	3506 (1)	41 (1)
O1	3410 (2)	1166 (1)	2469 (1)	50 (1)
O2	1741 (2)	4227 (1)	2091 (1)	50 (1)
O3	925 (2)	2157 (2)	2432 (1)	52 (1)
O4	3267 (2)	3341 (2)	2952 (1)	54 (1)
C1	4266 (2)	890 (2)	1930 (1)	39 (1)
C2	5134 (2)	−162 (2)	1882 (1)	42 (1)
C3	6015 (2)	−357 (2)	1289 (1)	46 (1)
C4	6109 (2)	418 (2)	721 (1)	41 (1)
C5	5278 (2)	1416 (2)	767 (1)	41 (1)
C6	4327 (2)	1689 (2)	1356 (1)	38 (1)
C7	5028 (2)	−1038 (2)	2474 (1)	53 (1)
C8	6090 (3)	−2071 (3)	2341 (2)	80 (1)
C9	5052 (3)	−536 (3)	3115 (1)	67 (1)
C10	3830 (3)	−1402 (3)	2584 (2)	73 (1)
C11	7159 (2)	124 (2)	90 (1)	49 (1)
C12	7306 (3)	−1080 (3)	−96 (2)	87 (2)
C13	6937 (3)	890 (3)	−514 (1)	87 (1)
C14	8318 (3)	236 (3)	225 (2)	82 (2)
C15	2131 (2)	4399 (2)	1451 (1)	39 (1)
C16	1656 (2)	5411 (2)	1105 (1)	45 (1)
C17	2138 (2)	5500 (2)	426 (1)	50 (1)
C18	3069 (2)	4665 (2)	48 (1)	45 (1)
C19	3516 (2)	3698 (2)	373 (1)	44 (1)
C20	3076 (2)	3530 (2)	1079 (1)	38 (1)
C21	665 (3)	6341 (2)	1505 (1)	61 (1)
C22	−423 (3)	5875 (3)	1918 (2)	83 (1)
C23	1215 (3)	6814 (3)	1970 (2)	83 (2)
C24	211 (3)	7306 (3)	1041 (2)	100 (2)
C25	3525 (3)	4854 (2)	−719 (1)	56 (1)
C26	2551 (4)	4715 (3)	−1034 (2)	88 (2)
C27	4716 (3)	4018 (3)	−1010 (2)	93 (2)
C28	3756 (3)	6033 (3)	−897 (2)	80 (2)
C29	174 (2)	1915 (2)	2985 (1)	44 (1)
C30	−792 (2)	1413 (2)	2991 (1)	52 (1)
C31	−1540 (3)	1205 (2)	3607 (2)	61 (1)
C32	−1406 (3)	1440 (2)	4228 (1)	60 (1)
C33	−475 (3)	1908 (2)	4222 (1)	56 (1)
C34	350 (2)	2169 (2)	3611 (1)	45 (1)
C35	−945 (3)	1118 (3)	2328 (2)	72 (1)
C36	−2034 (4)	559 (4)	2451 (2)	118 (2)
C37	−1152 (3)	2172 (4)	1871 (2)	93 (2)
C38	190 (3)	270 (3)	1984 (2)	94 (2)
C39	−2302 (3)	1160 (3)	4887 (2)	76 (1)
C40	−3514 (4)	1810 (6)	4918 (3)	244 (4)
C41	−2264 (6)	−64 (4)	4951 (3)	190 (4)
C42	−1950 (5)	1381 (7)	5487 (2)	220 (5)
C43	2867 (2)	3433 (2)	3587 (1)	43 (1)
C44	3452 (3)	3949 (2)	3953 (1)	52 (1)
C45	2969 (3)	3978 (2)	4631 (1)	60 (1)
C46	1921 (3)	3574 (3)	4988 (1)	61 (1)
C47	1349 (3)	3126 (2)	4642 (1)	58 (1)
C48	1787 (2)	3023 (2)	3936 (1)	46 (1)
C49	4535 (3)	4451 (3)	3573 (2)	67 (1)
C50	5583 (3)	3550 (4)	3201 (2)	94 (2)
C51	4124 (4)	5381 (3)	3072 (2)	93 (2)
C52	5007 (4)	4978 (4)	4049 (2)	108 (2)
C53	1470 (3)	3689 (3)	5754 (2)	82 (2)
C54	1338 (4)	4909 (4)	5919 (2)	112 (2)
C55	258 (5)	3387 (5)	6038 (2)	166 (4)
C56	2428 (4)	2907 (4)	6073 (2)	121 (2)

[a] Equivalent isotropic U defined as one-third of the trace of the orthogonalized U_{ij} tensor.

Table III. Atomic Coordinates ($\times 10^4$) and Equivalent Isotropic Displacement Parameters ($Å^2 \times 10^3$) for $Ni(C_{28}H_{40}NO_2)_2$

atom	x/a	y/b	z/c	U[a]
Ni1	5125 (1)	2340 (1)	2494 (1)	43 (1)
O1	6174 (2)	765 (2)	2153 (1)	52 (1)
O2	4059 (2)	3918 (2)	2519 (1)	50 (1)
O3	3663 (2)	1714 (2)	2910 (1)	54 (1)
O4	6636 (2)	2921 (2)	2378 (1)	56 (1)
N1	5072 (2)	2381 (2)	1527 (1)	39 (1)
N2	5146 (3)	2384 (2)	3465 (1)	43 (1)
C1	6406 (3)	617 (3)	1520 (2)	44 (1)
C2	7235 (3)	−398 (3)	1157 (2)	49 (1)
C3	7430 (3)	−479 (3)	481 (2)	54 (1)
C4	6888 (3)	360 (3)	95 (2)	49 (1)
C5	6131 (3)	1313 (3)	423 (2)	49 (1)
C6	5829 (3)	1483 (3)	1138 (2)	42 (1)
C7	7822 (4)	−1329 (3)	1554 (2)	66 (2)
C8	8756 (4)	−2291 (4)	1081 (2)	100 (2)
C9	6795 (5)	−1786 (3)	2013 (2)	87 (2)
C10	8499 (4)	−868 (4)	1979 (2)	90 (2)
C11	7221 (4)	167 (3)	−675 (2)	62 (2)
C12	8520 (5)	247 (5)	−979 (2)	106 (3)
C13	6350 (5)	1016 (4)	−977 (2)	109 (3)
C14	7113 (5)	−990 (4)	−852 (2)	88 (2)
C15	3780 (3)	4128 (3)	1974 (2)	41 (1)
C16	2953 (3)	5183 (3)	1901 (2)	44 (1)
C17	2693 (3)	5337 (3)	1299 (2)	49 (1)
C18	3175 (3)	4539 (3)	739 (2)	45 (1)
C19	3945 (3)	3558 (3)	796 (2)	44 (1)
C20	4299 (3)	3307 (3)	1400 (2)	42 (1)
C21	2461 (3)	6079 (3)	2483 (2)	56 (2)
C22	3541 (4)	6451 (3)	2597 (2)	78 (2)
C23	1786 (4)	5624 (3)	3129 (2)	71 (2)
C24	1552 (4)	7097 (3)	2323 (2)	83 (2)
C25	2770 (3)	4818 (3)	94 (2)	52 (1)
C26	2903 (5)	5973 (4)	−115 (2)	89 (2)
C27	1447 (4)	4772 (4)	231 (2)	86 (2)
C28	3564 (4)	4006 (4)	−492 (2)	91 (2)
C29	3500 (3)	1589 (3)	3531 (2)	46 (1)
C30	2567 (3)	1057 (3)	3908 (2)	53 (1)
C31	2399 (4)	1011 (3)	4582 (2)	61 (2)
C32	3086 (4)	1424 (3)	4944 (2)	62 (2)
C33	3993 (4)	1877 (3)	4596 (2)	62 (2)
C34	4256 (3)	1983 (3)	3883 (2)	47 (1)
C35	1869 (4)	528 (4)	3531 (2)	71 (2)
C36	973 (5)	−33 (5)	4002 (2)	111 (3)
C37	2802 (5)	−360 (4)	3007 (2)	100 (3)
C38	1136 (4)	1417 (5)	3175 (2)	96 (2)
C39	2789 (4)	1303 (4)	5706 (2)	81 (2)
C40	2791 (5)	100 (5)	5871 (2)	117 (3)
C41	1508 (5)	2051 (5)	6034 (2)	115 (3)
C42	3704 (6)	1642 (7)	5996 (2)	157 (5)
C43	6812 (3)	3117 (3)	2940 (2)	48 (1)
C44	7789 (3)	3610 (3)	2966 (2)	55 (2)
C45	7917 (4)	3791 (3)	3589 (2)	64 (2)
C46	7145 (4)	3545 (3)	4208 (2)	62 (2)
C47	6236 (4)	3076 (3)	4188 (2)	58 (2)
C48	6008 (3)	2841 (3)	3567 (2)	47 (1)
C49	8610 (4)	3922 (4)	2312 (2)	79 (2)
C50	7834 (5)	4771 (4)	1971 (2)	99 (3)
C51	9274 (4)	2880 (5)	1842 (2)	100 (3)
C52	9582 (5)	4445 (5)	2451 (3)	124 (4)
C53	7401 (5)	3821 (4)	4872 (2)	80 (2)
C54	6453 (7)	3563 (7)	5476 (3)	181 (5)
C55	8637 (6)	3160 (6)	4880 (3)	197 (4)
C56	7285 (7)	5043 (5)	4945 (3)	160 (5)

[a] Equivalent isotropic U defined as one-third of the trace of the orthogonalized U_{ij} tensor.

is Fe^{III}(Cat-N-BQ)(Cat-N-SQ) with mixed-charge ligands. The magnetic moment reported for the complex of 5.33 μ_B could be associated with high-spin Fe(II), but in this case it must arise from antiferromagnetic coupling between the $S = {}^5/_2$ ferric ion and the radical Cat-N-SQ^{2-} ligand.

Structural Features of Fe(Cat-N-BQ)(Cat-N-SQ) and Ni(Cat-N-BQ)$_2$. The two biquinone ligands of the Fe and Ni complexes chelate at meridional sites of an octahedron. Drawings of both complex molecules are given in Figure 1, and bond distances and angles are given in Tables IV and V. Average M–O and M–N lengths of the two metals are consistent with their charges and are, generally, longer than corresponding values of the Co and Mn molecules given in Table VI. As with the Co and Mn structures, one ligand of Fe(Cat-N-BQ)(Cat-N-SQ) and of Ni(Cat-N-BQ)$_2$ shows a marked deviation from planarity. The dihedral angles between ring planes of the ligands in both structures that contain O1, N1, and O2 are 12.6° (Ni) and 11.7° (Fe); the second ligands (O3, N2, O4) in both structures are closer

Table IV. Bond Distances and Angles for $Fe(C_{28}H_{40}NO_2)_2$

Distances (Å)			
Fe–N1	2.108 (2)	Fe–N2	2.126 (2)
Fe–O1	1.988 (2)	Fe–O2	1.997 (2)
Fe–O3	1.981 (2)	Fe–O4	1.983 (2)
N1–C6	1.358 (3)	N1–C20	1.361 (3)
N2–C34	1.354 (4)	N2–C48	1.356 (4)
O1–C1	1.290 (2)	O2–C15	1.291 (3)
O3–C29	1.292 (3)	O4–C43	1.278 (3)
C1–C2	1.427 (3)	C1–C6	1.453 (3)
C2–C3	1.369 (3)	C3–C4	1.425 (3)
C4–C5	1.357 (3)	C5–C6	1.414 (3)
C15–C16	1.430 (3)	C15–C20	1.446 (3)
C16–C17	1.368 (3)	C17–C18	1.418 (3)
C18–C19	1.359 (3)	C19–C20	1.421 (3)
C29–C30	1.418 (4)	C29–C34	1.454 (4)
C30–C31	1.371 (4)	C31–C32	1.415 (5)
C32–C33	1.355 (5)	C33–C34	1.423 (3)
C43–C44	1.442 (4)	C43–C48	1.452 (4)
C44–C45	1.365 (4)	C45–C46	1.420 (4)
C46–C47	1.351 (5)	C47–C48	1.421 (3)
Angles (deg)			
N1–Fe–N2	175.0 (1)	N1–Fe–O1	77.3 (1)
N2–Fe–O1	97.7 (1)	N1–Fe–O2	77.2 (1)
N2–Fe–O2	107.8 (1)	O1–Fe–O2	154.6 (1)
N1–Fe–O3	102.2 (1)	N2–Fe–O3	77.3 (1)
O1–Fe–O3	93.5 (1)	O2–Fe–O3	92.8 (1)
N1–Fe–O4	103.7 (1)	N2–Fe–O4	77.1 (1)
O1–Fe–O4	94.4 (1)	O2–Fe–O4	90.6 (1)
O3–Fe–O4	154.0 (1)	Fe–N1–C6	114.6 (1)
Fe–N1–C20	114.4 (1)	C6–N1–C20	131.0 (2)
Fe–N2–C34	114.1 (2)	Fe–N2–C48	114.3 (2)
C34–N2–C48	131.6 (2)	Fe–O1–C1	118.0 (1)
Fe–O2–C15	117.5 (1)	Fe–O3–C29	118.3 (2)
Fe–O4–C43	118.4 (2)	O1–C1–C2	122.5 (2)
O1–C1–C6	117.9 (2)	C2–C1–C6	119.6 (2)
C1–C2–C3	117.5 (2)	C1–C2–C7	119.8 (2)
C3–C2–C7	122.7 (2)	C2–C3–C4	124.1 (2)
C3–C4–C5	118.3 (2)	C3–C4–C11	119.6 (2)
C5–C4–C11	122.1 (2)	C4–C5–C6	121.8 (2)
N1–C6–C1	111.6 (2)	N1–C6–C5	129.6 (2)
C1–C6–C5	118.7 (2)	O2–C15–C16	122.2 (2)
O2–C15–C20	118.2 (2)	C16–C15–C20	119.6 (2)
C15–C16–C17	117.1 (2)	C15–C16–C21	119.4 (2)
C17–C16–C21	123.5 (2)	C16–C17–C18	124.6 (2)
C17–C18–C19	118.5 (2)	C17–C18–C25	119.9 (2)
C19–C18–C25	121.6 (2)	C18–C19–C20	120.9 (2)
N1–C20–C15	111.8 (2)	N1–C20–C19	129.0 (2)
C15–C20–C19	119.2 (2)	O3–C29–C30	121.7 (2)
O3–C29–C34	117.9 (2)	C30–C29–C34	120.4 (2)
C29–C30–C31	116.7 (3)	C29–C30–C35	119.8 (2)
C31–C30–C35	123.5 (3)	C30–C31–C32	125.0 (3)
C31–C32–C33	118.3 (2)	C31–C32–C39	120.1 (3)
C33–C32–C39	121.6 (3)	C32–C33–C34	121.5 (3)
N2–C34–C29	112.0 (2)	N2–C34–C33	129.8 (3)
C29–C34–C33	118.2 (3)	O4–C43–C44	121.5 (2)
O4–C43–C48	118.5 (3)	C44–C43–C48	120.0 (2)
C43–C44–C45	116.7 (3)	C43–C44–C49	119.6 (2)
C45–C44–C49	123.7 (3)	C44–C45–C46	124.6 (3)
C45–C46–C47	118.7 (2)	C45–C46–C53	118.5 (3)
C47–C46–C53	122.8 (3)	C46–C47–C48	121.8 (3)
N2–C48–C43	111.6 (2)	N2–C48–C47	130.2 (3)
C43–C48–C47	118.2 (3)		

Table V. Bond Distances and Angles for $Ni(C_{28}H_{40}NO_2)_2$

Distances (Å)			
Ni–O1	2.042 (2)	Ni–O2	2.029 (2)
Ni–O3	2.022 (3)	Ni–O4	2.024 (3)
Ni–N1	2.019 (3)	Ni–N2	2.019 (3)
O1–C1	1.268 (4)	O2–C15	1.267 (4)
O3–C29	1.259 (4)	O4–C43	1.273 (4)
N1–C6	1.344 (3)	N1–C20	1.343 (4)
N2–C34	1.350 (4)	N2–C48	1.338 (5)
C1–C2	1.449 (4)	C1–C6	1.462 (5)
C2–C3	1.353 (5)	C2–C7	1.537 (5)
C3–C4	1.430 (5)	C4–C5	1.343 (4)
C4–C11	1.540 (5)	C5–C6	1.429 (4)
C15–C16	1.450 (4)	C15–C20	1.462 (4)
C16–C17	1.364 (5)	C16–C21	1.532 (5)
C17–C18	1.425 (4)	C18–C19	1.344 (4)
C18–C25	1.543 (5)	C19–C20	1.431 (5)
C29–C30	1.450 (5)	C29–C34	1.462 (6)
C30–C31	1.356 (5)	C30–C35	1.531 (7)
C31–C32	1.423 (7)	C32–C33	1.348 (6)
C32–C39	1.531 (5)	C33–C34	1.431 (5)
C43–C44	1.438 (6)	C43–C48	1.468 (4)
C44–C45	1.366 (6)	C44–C49	1.532 (6)
C45–C46	1.424 (5)	C46–C47	1.344 (7)
C46–C53	1.548 (7)	C48–C48	1.431 (6)
Angles (deg)			
O1–Ni–O2	161.3 (1)	O1–Ni–O3	89.8 (1)
O2–Ni–O3	93.2 (1)	O1–Ni–O4	91.9 (1)
O2–Ni–O4	91.0 (1)	O3–Ni–O4	161.8 (1)
O1–Ni–N1	80.6 (1)	O2–Ni–N1	80.8 (1)
O3–Ni–N1	99.9 (1)	O4–Ni–N1	98.3 (1)
O1–Ni–N2	102.2 (1)	O2–Ni–N2	96.5 (1)
O3–Ni–N2	81.0 (1)	O4–Ni–N2	80.9 (1)
N1–Ni–N2	177.1 (1)	Ni–O4–C43	112.3 (2)
Ni–N1–C6	113.6 (2)	Ni–N1–C20	113.5 (2)
C6–N1–C20	132.9 (3)	Ni–N2–C34	113.2 (3)
Ni–N2–C48	113.7 (2)	C34–N2–C48	133.0 (3)
Ni–O1–C1	112.0 (2)	Ni–O2–C15	112.1 (2)
Ni–O3–C29	112.6 (3)	O1–C1–C2	121.8 (3)
O1–C1–C6	120.0 (2)	C2–C1–C6	118.3 (3)
C1–C2–C3	117.5 (3)	C1–C2–C7	118.9 (3)
C3–C2–O7	123.6 (3)	C2–C3–C4	125.3 (3)
C3–C4–C5	118.0 (3)	C3–C4–C11	119.7 (3)
C5–C4–C11	122.3 (3)	C4–C5–C6	121.8 (3)
N1–C6–C1	113.0 (3)	N1–C6–C5	127.9 (3)
C1–C6–C5	119.1 (3)	O2–C15–C16	121.1 (3)
O2–C15–C20	120.2 (3)	C16–C15–C20	118.7 (3)
C15–C16–C17	117.3 (3)	C15–C16–C21	119.3 (3)
C17–C16–C21	123.4 (3)	C16–C17–C18	124.7 (3)
C17–C18–C19	118.8 (3)	C17–C18–C25	118.9 (3)
C19–C18–C25	122.2 (3)	C18–C19–C20	121.5 (3)
N1–C20–C15	112.8 (3)	N1–C20–C19	128.3 (3)
C15–C20–C19	118.9 (3)	O3–C29–C30	120.8 (4)
O3–C29–C34	120.1 (3)	C30–C29–C34	119.1 (3)
C29–C30–C31	117.3 (4)	C29–C30–C35	119.4 (3)
C31–C30–C35	123.2 (4)	C30–C31–C32	125.0 (4)
C31–C32–C33	118.3 (3)	C31–C32–C39	118.7 (4)
C33–C32–C39	123.0 (4)	C32–C33–C34	122.2 (4)
N2–C34–C29	112.9 (3)	N2–C34–C33	129.0 (4)
C29–C34–C33	118.0 (3)	C30–C35–C36	111.9 (4)
C30–C35–C37	108.8 (4)	O4–C43–C44	120.7 (3)
O4–C43–C48	119.7 (4)	C44–C43–C48	119.6 (3)
C43–C44–C45	117.0 (3)	C43–C44–C49	119.5 (4)
C45–C44–C49	123.4 (4)	C44–C45–C46	124.8 (4)
C45–C46–C47	118.6 (4)	C45–C46–C53	118.4 (4)
C47–C46–C53	123.0 (3)	C46–C47–C48	122.0 (3)
N2–C48–C43	113.0 (3)	N2–C48–C47	129.1 (3)
C43–C48–C47	117.9 (4)		

to planarity with dihedral angles of 4.9° for each. The average Fe–N and Fe–O lengths are 2.117 (2) and 1.987 (2) Å; the average Ni–N and Ni–O values are 2.031 (2) and 2.019 (3) Å. Even though the ligands of the iron complex are of mixed charge, the electronic difference is not reflected in their structural parameters and the thermal parameters of the ligand atoms do not suggest structural disorder. All four C–O and C–N lengths of the iron molecule show consistency with average values of 1.287 (3) and 1.357 (3) Å, respectively. Corresponding lengths of the nickel complex are slightly shorter, 1.264 (5) and 1.344 (5) Å, in accord with the lower overall ligand charge in this molecule. Average C–O and C–N lengths of the Co and Mn complexes are given in Table VI. The cobalt values are similar to the iron lengths, the manganese values are the longest of the series, and the pattern of increasing C–O and C–N lengths with increasing ligand charge is subtle but clear. Further, differences in overall ligand charge for the complexes of this series appear in the ring C–C lengths. The expectation is that as the extent of ligand reduction increases, the rings should become increasingly aromatic to the point where the Cat-N-Cat^{3-} form not observed for this series should have essentially identical ring lengths. Lengths at ring bonds 3 and 5 in the drawing given with Table VI should be particularly

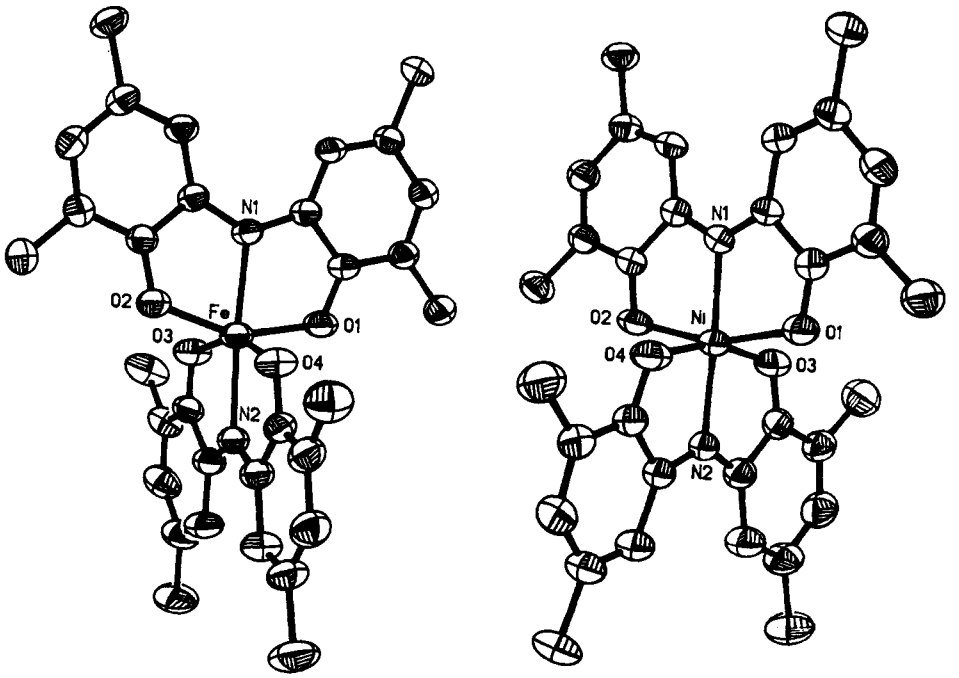

Figure 1. Views of the $Ni(Cat\text{-}N\text{-}BQ)_2$ and $Fe(Cat\text{-}N\text{-}BQ)(Cat\text{-}N\text{-}SQ)$ complex molecules.

Table VI. Metal and Ligand Bond Lengths (Å) for the Three Tautomeric Forms in the Bis(biquinone) Complexes

	$Mn(Cat\text{-}N\text{-}SQ)_2$	$Co(Cat\text{-}N\text{-}BQ)(Cat\text{-}N\text{-}SQ)$	$Fe(Cat\text{-}N\text{-}BQ)(Cat\text{-}N\text{-}SQ)$	$Ni(Cat\text{-}N\text{-}BQ)_2$
M–O	1.896 (5)	1.896 (5)	1.987 (2)	2.031 (2)
M–N	1.910 (5	1.868 (5)	2.117 (2)	2.019 (3)
C–O	1.325 (7)	1.305 (7)	1.287 (3)	1.264 (5)
C–N	1.380 (7)	1.361 (6)	1.357 (3)	1.344 (5)
$C\text{–}C_1$[a]	1.417 (8)	1.445 (7)	1.452 (3)	1.464 (4)
$C\text{–}C_2$	1.408 (8)	1.450 (7)	1.430 (3)	1.450 (4)
$C\text{–}C_3$	1.380 (9)	1.376 (7)	1.368 (4)	1.353 (4)
$C\text{–}C_4$	1.412 (8)	1.416 (7)	1.420 (4)	1.429 (4)
$C\text{–}C_5$	1.367 (8)	1.360 (7)	1.355 (3)	1.344 (4)
$C\text{–}C_6$	1.410 (9)	1.419 (7)	1.420 (3)	1.430 (4)

[a] Ligand bond notation:

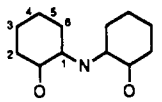

sensitive to ligand charge with double bond values for the fully oxidized $BQ\text{-}N\text{-}BQ^+$ form. Even for $Mn^{IV}(Cat\text{-}N\text{-}SQ)_2$, with the most reduced ligands of the series, the average C–C bond lengths at these positions are shorter than other ring values. Extending across the series to $Ni^{II}(Cat\text{-}N\text{-}BQ)_2$, there is pronounced shortening of bonds at the 3- and 5-positions and lengthening of other ring bonds. Structural features of the biquinone ligands, as with the quinones, appear to provide information on ligand charge.

Electrochemical Properties of the Schiff Base Biquinone Complexes. From the various electronic forms of the biquinone ligand, ligand-based electrochemical activity would be expected for the bis(biquinone) complexes. In cases where the metal ion is also electrochemically active, both metal and ligand redox processes may be observed.

Ligand-based electrochemistry was studied in complexes of redox inactive metals, and these results are given in Table VII and Figure 2. The magnesium, zinc, and nickel complexes, $M^{II}(Cat\text{-}N\text{-}BQ)_2$, M = Mg, Zn, and Ni, show two reversible or quasireversible reductions at approximately −1.2 and −1.5 V (vs Fc/Fc^+), an additional irreversible reduction at −2.2 V (except Ni), a reversible oxidation at +0.33 V, and a second oxidation at +0.69 V. All are one-electron processes. Oxidation must result in formation of the radical SQ-N-BQ ligand at the metals, the two reversible reduction processes result in the $M(Cat\text{-}N\text{-}SQ)_2^{2-}$ form of the complexes, and further reduction must result in the reactive $Cat\text{-}N\text{-}Cat^{3-}$ form of the ligand (eq 1). EPR spectra

$$M(SQ\text{-}N\text{-}BQ)_2^{2+} \overset{e^-}{\rightleftharpoons} M(SQ\text{-}N\text{-}BQ)(Cat\text{-}N\text{-}BQ)^+ \overset{e^-}{\rightleftharpoons} M(Cat\text{-}N\text{-}BQ)_2 \overset{e^-}{\rightleftharpoons} M(Cat\text{-}N\text{-}BQ)(Cat\text{-}N\text{-}SQ)^- \overset{e^-}{\rightleftharpoons} M(Cat\text{-}N\text{-}SQ)_2^{2-} \overset{e^-}{\longrightarrow} M(Cat\text{-}N\text{-}SQ)(Cat\text{-}N\text{-}Cat)^{3-} \quad (1)$$

on the copper complex confirm that it also contains the divalent form of the metal ion, $Cu^{II}(Cat\text{-}N\text{-}BQ)_2$.[2] It, also, undergoes oxidation and reduction reactions that are similar to those of the Mg, Zn, and Ni series. However, the first oxidation potential is more negative by 0.2 V, the first reduction is 0.2 V more positive, and the second and third reductions occur at similar potentials near −1.55 V. This behavior is clearly different from that of the other members of the series and merits further study.

A negative shift in the first oxidation potential and a positive shift in the second is observed with the change in charge distribution to $M^{III}(Cat\text{-}N\text{-}BQ)(Cat\text{-}N\text{-}SQ)$ for the Fe and Co com-

Table VII. Voltammetric Redox Processes for the Bis(biquinone) Complexes

	$E°$,[a] V(ΔE_p, mV)				
	oxdn 2	oxdn 1	redn 1	redn 2	redn 3
$Mg(Cat\text{–}N\text{–}BQ)_2$	0.69[b]	0.32 (81)	−1.22 (82)	−1.51 (91)	−2.32[b]
$Zn(Cat\text{–}N\text{–}BQ)_2$	0.68 (121)	0.34 (73)	−1.17 (72)	−1.50 (87)	−2.21[b]
$Ni(Cat\text{–}N\text{–}BQ)_2$	0.70 (71)	0.33 (71)	−1.20 (71)	−1.53 (73)	
$Cu(Cat\text{–}N\text{–}BQ)_2$	0.85 (120)	0.13 (71)	−0.97 (89)	−1.52, −1.60 (287)	
$Fe(Cat\text{–}N\text{–}BQ)(Cat\text{–}N\text{–}SQ)$	1.09 (73)	−0.14 (72)	−0.77 (76)	−1.60 (79)	−2.01 (88)
$Co(Cat\text{–}N\text{–}BQ)(Cat\text{–}N\text{–}SQ)$	1.16 (95)	−0.36 (89)	−0.91 (97)	−1.77 (163)	−2.36[b]
$Mn(Cat\text{–}N\text{–}SQ)_2$	1.02 (119)	0.20 (92)	−0.99 (125)	−1.55 (137)	−2.44[b]

[a] $E°$ values recorded at scan rates of 100 mV/s and referenced to the Fc/Fc^+ couple. [b] Irreversible.

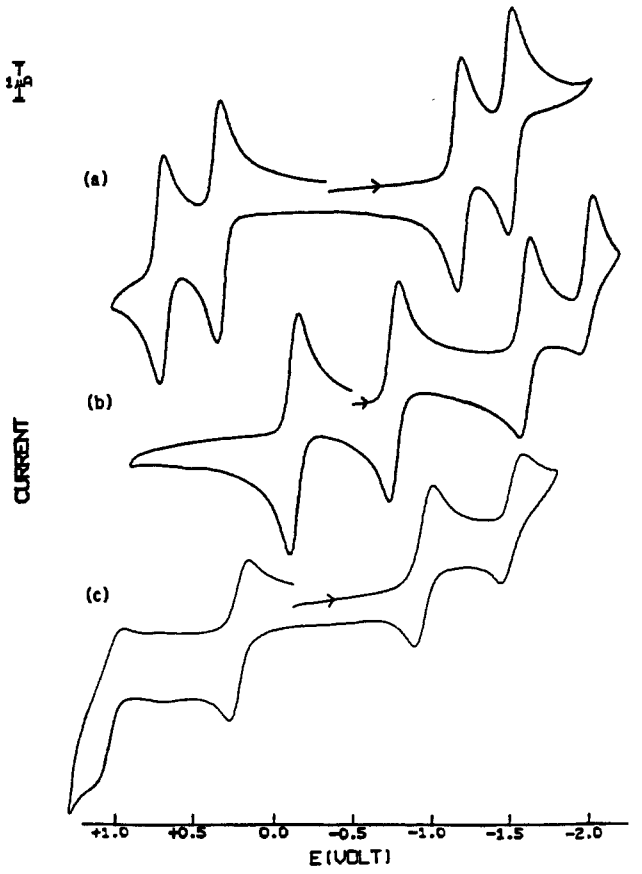

Figure 2. Cyclic voltammograms, showing the oxidation and reduction couples for (a) Ni(Cat-N-BQ)$_2$, (b) Fe(Cat-N-BQ)(Cat-N-SQ), and (c) Mn(Cat-N-SQ)$_2$. Potentials are referenced to the Fc/Fc$^+$ couple.

plexes. Oxidation of these complexes occurs at the ligands (eq 2). Reduction may occur at either the metal (eq 3) or at the

$$M(SQ\text{-}N\text{-}BQ)(Cat\text{-}N\text{-}BQ)^{2+} \overset{e^-}{\rightleftharpoons} M(Cat\text{-}N\text{-}BQ)_2^{+} \overset{e^-}{\rightleftharpoons} M(Cat\text{-}N\text{-}BQ)(Cat\text{-}N\text{-}SQ) \quad (2)$$

$$M^{III}(Cat\text{-}N\text{-}BQ)(Cat\text{-}N\text{-}SQ) \overset{e^-}{\rightleftharpoons} M^{II}(Cat\text{-}N\text{-}BQ)(Cat\text{-}N\text{-}SQ)^{-} \overset{e^-}{\rightleftharpoons} M^{II}(Cat\text{-}N\text{-}SQ)_2^{2-} \overset{e^-}{\longrightarrow} M^{II}(Cat\text{-}N\text{-}SQ)(Cat\text{-}N\text{-}Cat)^{3-} \quad (3)$$

$$M^{III}(Cat\text{-}N\text{-}BQ)(Cat\text{-}N\text{-}SQ) \overset{e^-}{\rightleftharpoons} M(Cat\text{-}N\text{-}SQ)_2^{-} \overset{e^-}{\rightleftharpoons} M(Cat\text{-}N\text{-}SQ)(Cat\text{-}N\text{-}Cat)^{2-} \overset{e^-}{\longrightarrow} M(Cat\text{-}N\text{-}Cat)_2^{3-} \quad (4)$$

ligands (eq 4). The first reductions are slightly more positive than the corresponding reductions of the M(II) complexes, and the second reduction is shifted to slightly more negative potentials. This similarity with the electrochemistry of the M^{II}(Cat-N-BQ)$_2$ series may point to the ligand-based redox activity shown in reaction 4, but there is no strong evidence that differentiates between the two types of processes.

The question of metal- or ligand-based redox activity is complicated further by the manganese complex. The cyclic voltammogram of this complex is strikingly similar to the CV's of the M^{II}(Cat-N-BQ)$_2$ complexes. Potentials for the oxidation and reduction processes are given in Table VII. In an earlier investigation we noted that *trans*-Mn^{IV}(py)$_2$(DBCat)$_2$ existed in the Mn(IV) form in solid state and in solution at low temperature.[7] However, in toluene solution, as solution temperature was increased from −40 °C, an equilibrium between purple Mn(IV) and green Mn(II) forms was observed to occur with forms of the complex related by intramolecular transfer of electrons between the metal and the quinone ligands (eq 5). At room temperature the complex

$$Mn^{IV}(py)_2(DBCat)_2 \rightleftarrows Mn^{II}(py)_2(DBSQ)_2 \quad (5)$$

existed in solution entirely in the Mn(II) form. A similar equilibrium is possible for Mn^{IV}(Cat-N-SQ)$_2$ (eq 6). However,

$$Mn^{IV}(Cat\text{-}N\text{-}SQ)_2 \rightleftarrows Mn^{II}(Cat\text{-}N\text{-}BQ)_2 \quad (6)$$

electronic spectra recorded on the complex in solid state are similar to solution spectra, including characteristic charge-transfer bands in the near-infrared region, and the complex appears to retain its solid-state charge distribution in solution. Oxidation of the complex probably occurs at the ligands to give Mn^{IV}(Cat-N-BQ)(Cat-N-SQ)$^+$ and Mn^{IV}(Cat-N-BQ)$_2^{2+}$, with charge distributions that are similar to species associated with the other redox series. The three reduction steps occur at potentials that are not significantly different from those of the reduction processes of the M(II) series. However, only two units of charge would be required to give the form of the complex with fully reduced Cat-N-Cat^{3-} ligands, and one of the reduction steps must occur at the metal. We speculated earlier, on the basis of the unusually high oxidation state of the metal in this complex and the accessibility of Mn(III) and Mn(II) forms of the metal, that the first two reductions occurred at the metal to give Mn^{III}(Cat-N-SQ)$_2^-$ and Mn^{II}(Cat-N-SQ)$_2^{2-}$. This may be the case, but, in view of the electrochemistry of the M^{II}(Cat-N-BQ)$_2$ series, other options are clearly possible.

Discussion

The Schiff base biquinone ligand may chelate with metal ions in a number of charged forms. Products obtained from the electrochemical reactions described above contain ligands ranging in charge from the neutral BQ-N-SQ form resulting from oxidation of the M^{II}(Cat-N-BQ)$_2$ series to the Cat-N-Cat^{3-} ligand present in the fully reduced form of the manganese complex. Ligand and metal charge in the biquinone complexes often requires definition. The M(II) form of the metal is the only reasonable oxidation state for the Mg, Zn, Ni, and Cu complexes, and the magnetic and EPR properties of the Ni and Cu complexes further point to the divalent form of the metal ions. Other charge distributions are available as options for the complexes prepared with the redox-active metal ions Fe^{2+}, Co^{2+}, and Mn^{2+}, and magnetic coupling between radical forms of the ligand and the paramagnetic metal may complicate interpretation of magnetic properties. Cobalt–oxygen and Co–N bond lengths indicated Co(III), and the radical EPR spectrum weakly coupled to the ^{59}Co nucleus and a single ring proton were consistent with the Co^{III}(Cat-N-BQ)(Cat-N-SQ) charge distribution. The manganese complex also was found to have one unpaired electron, but in this case the EPR spectrum indicated that spin density was concentrated on the metal. Mn–N and Mn–O lengths pointed to Mn(IV), and the $S = {}^1/_2$ magnetic ground state must result from strong spin coupling between the $S = {}^3/_2$ metal and the two radical ligands. The iron complex, reported initially by Balch, shows a Mössbauer spectrum that indicates Fe(III), and the $S = 2$ magnetic moment of the complex arises from coupling of the $S = {}^5/_2$ metal with the single radical ligand of Fe^{III}(Cat-N-BQ)(Cat-N-SQ).

With structural information available for the three types of complexes, bond lengths contained in Table VI can be used as an indication of ligand charge in cases where esd's permit comparison. The variation in individual bond lengths is small, but the tendency toward increased *o*-benzoquinone character for the rings as ligand oxidation increases is clear from the collective variation in C–C, C–O, and C–N lengths for the series. In particular, as the extent of ligand oxidation increases, ring bonds at the 3- and 5-positions approach double-bond values and the multiple character reflected in the C–N and C–O bond lengths increases. As with the semiquinone and catecholate complexes, ligand structural features of the biquinone complexes may be used

(7) Lynch, M. W.; Hendrickson, D. N.; Fitzgerald, B. J.; Pierpont, C. G. *J. Am. Chem. Soc.* **1984**, *106*, 2041.

to provide information on charge distribution.

Acknowledgment. This research was supported by the National Science Foundation under Grant CHE 88-09923. We thank Professor D. N. Hendrickson for providing the Mössbauer spectrum of Fe(Cat-N-BQ)(Cat-N-SQ).

Supplementary Material Available: For both Fe(Cat-N-BQ)(Cat-N-SQ) and Ni(Cat-N-BQ)$_2$, tables listing crystal data and details of the structure determinations, anisotropic thermal parameters, and hydrogen atom locations (11 pages); listings of observed and calculated structure factors (85 pages). Ordering information is given on any current masthead page.

Contribution from the Department of Chemistry, Harvard University, Cambridge, Massachusetts 02138

Aspects of the Oxygen Atom Transfer Chemistry of Tungsten

Shi-bao Yu and R. H. Holm*

Received March 6, 1989

The oxygen atom transfer chemistry of most elements that form stable metal–oxo compounds, among them tungsten, is unsystematically developed at present. Reported here are certain aspects of the oxo transfer chemistry of tungsten Schiff base and N,N-disubstituted dithiocarbamate (R_2dtc) complexes, which are compared with the far more extensively examined chemistry of molybdenum with these ligands. A reproducible preparation of $WO_2(acac)_2$ (**4**, acac = acetylacetonate(1−)) is described. Compound **4** and the Schiff bases H_2(sap) and H_2(ssp) afford the complexes WO_2(sap) (**5**, sap = 2-(salicylideneamino)-phenolate(2−)), WO_2(5-*t*-Busap) (**6**), and WO_2(ssp) (**7**, ssp = 2-(salicylideneamino)benzenethiolate(2−)). When recrystallized from methanol, **6** gave [WO_2(5-*t*-Busap)(MeOH)]·MeOH, which was obtained in monoclinic space group $P2_1$ with a = 6.832 (2) Å, b = 11.299 (4) Å, c = 13.354 (7) Å, β = 99.02 (4)°, and Z = 2. With use of 2997 unique data ($I > 3\sigma(I)$), the structure was refined to R (R_w) = 3.50% (4.80%). The complex contains a *cis*-dioxo group, a coordinated methanol molecule trans to one oxo ligand, and a *mer* arrangement of the tridentate ligand, whose oxygen atoms are mutually trans and are cis to the oxo ligands. The two W=O bond lengths differ by 0.12 Å. In contrast to their Mo analogues, **6–8** are unreactive to reductive oxo transfer with a number of basic tertiary phosphines under moderately forcing conditions. The compounds do undergo O/S substitution with $(Me_3Si)_2S$, yielding WS_2(sap) and WS_2(ssp). The $Mo^{VI}S_2$ *group* is unknown. Reactions of $W(CO)_3(R_2dtc)_2$ with $Mo_2O_3(Et_2dtp)_4$ (**14**, Et_2dtp = *O,O'*-diethyl dithiophosphate(1−)) afford in high yield $WO_2(R_2dtc)_2$ (R = Me, R_2 = $(CH_2)_5$ (**11**)) in examples of intermetal oxo transfer reactions. These compounds are much less stable than their Mo analogues and are very sensitive to water and dioxygen. The probable oxo donor is $MoO_2(Et_2dtp)_2$ (**16**), known to be in equilibrium with **14** and $MoO(Et_2dtp)_2$, which was isolated from the reaction. Compound **11** is unreactive to Ph_3P, in distinction to its Mo counterpart, which is relatively rapidly reduced in a strongly exothermic reaction. However, **11** is cleanly reduced by $(MeO)_3P$ to W_2O_3-$((CH_2)_5dtc)_4$. The reaction sequence presumably follows that in Mo systems, viz., reduction to the $W^{IV}O$ complex followed by a fast reaction of this species with the starting complex to afford the μ-oxo $W^{V}_2O_3$ product. Certain thermodynamic features of these reactions are discussed, and it is shown that, in terms of a previously introduced oxo transfer reactivity scale, **16** is a moderately strong oxo donor. The collective observations reflect a greater thermodynamic barrier to the reduction of W(VI) vs Mo(VI). Accordingly, $W^{IV}O$ complexes, unless stabilized by π-acid ligands, should be strong oxo acceptors. Recent reports of the initial cases of $W^{IV} \rightarrow W^{VI}$ oxo transfer reactions are considered in terms of the reactivity scale.

Introduction

Of all elements, the oxygen atom transfer chemistry of molybdenum is the most extensively investigated and best understood. Comprehensive accounts of Mo-mediated oxo transfer reactions are available.[1,2] Our research in this field[2-10] has been motivated by the problem of the mechanism of action of a broad class of enzymes, the molybdenum oxotransferases (hydroxylases).[11,12] The two most widespread transformations are the primary oxo transfer reaction[1] (1), wherein XO/X functions as an oxo donor/acceptor and the oxidation state of the Mo atom is changed by 2 units, and the μ-oxo dimerization reaction (2).

$$Mo^{VI}O_2L_n + X \rightleftharpoons Mo^{IV}OL_n + XO \quad (1)$$

$$Mo^{VI}O_2L_n + Mo^{IV}OL_n \rightleftharpoons Mo^{V}_2O_3L_{2n} \quad (2)$$

For reaction 1 and similar processes, a thermodynamic reactivity scale for substrates X/XO has been devised.[1,5] Reaction 2 is a reversible equilibrium when L is a N,N-disubstituted dithiocarbamate or related chelating monoanionic sulfur ligand,[1,13] but more frequently it is an irreversible process. This reaction occurs unless it is impeded by the steric properties of the ligand[4-9,14] or unless the Mo(IV) product of reaction 1 is trapped by added ligand.[10,15,16] Ligand systems that have figured prominently in the oxo-transfer chemistry of molybdenum include the dithiocarbamates,[1] the sterically bulky tridentates[17] L-NS_2[4-9] and $HB(Me_2pz)_3$,[14] and the tridentate Schiff bases sap and ssp.[10,15,18,19]

Our recent analysis of metal-mediated oxo transfer reactions[1] makes evident the lack of systematic development of the atom

(1) Holm, R. H. *Chem. Rev.* **1987**, *87*, 1401.
(2) Holm, R. H. *Coord. Chem. Rev.*, in press.
(3) Reynolds, M. S.; Berg, J. M.; Holm, R. H. *Inorg. Chem.* **1984**, *23*, 3057.
(4) Berg, J. M.; Holm, R. H. *J. Am. Chem. Soc.* **1985**, *107*, 917, 925.
(5) Harlan, E. W.; Berg, J. M.; Holm, R. H. *J. Am. Chem. Soc.* **1986**, *108*, 6992.
(6) Caradonna, J. P.; Harlan, E. W.; Holm, R. H. *J. Am. Chem. Soc.* **1986**, *108*, 7856.
(7) Holm, R. H.; Berg, J. M. *Acc. Chem. Res.* **1986**, *19*, 363.
(8) Caradonna, J. P.; Reddy, P. R.; Holm, R. H. *J. Am. Chem. Soc.* **1988**, *110*, 2139.
(9) Craig, J. A.; Holm, R. H. *J. Am. Chem. Soc.* **1989**, *111*, 2111.
(10) Craig, J. A.; Harlan, E. W.; Snyder, B. S.; Whitener, M. A.; Holm, R. H. *Inorg. Chem.* **1989**, *28*, 2082.
(11) *Molybdenum Enzymes*; Spiro, T. G., Ed.; Wiley-Interscience: New York, 1985.
(12) Bray, R. C. *Q. Rev. Biophys.* **1988**, *21*, 299.
(13) (a) Matsuda, T.; Tanaka, K.; Tanaka, T. *Inorg. Chem.* **1979**, *18*, 454. (b) Tanaka, T.; Tanaka, K.; Matsuda, T.; Hashi, K. In *Molybdenum Chemistry of Biological Significance*; Newton, W. E., Otsuka, S., Eds.; Plenum: New York, 1980; pp 361–367.
(14) Roberts, S. A.; Young, C. G.; Cleland, W. E., Jr.; Ortega, R. B.; Enemark, J. H. *Inorg. Chem.* **1988**, *27*, 3044.
(15) Boyd, I. W.; Spence, J. T. *Inorg. Chem.* **1982**, *21*, 1602.
(16) Kaul, B. B.; Enemark, J. H.; Merbs, S. L.; Spence, J. T. *J. Am. Chem. Soc.* **1985**, *107*, 2885.
(17) Abbreviations: acac, acetylacetonate(1−); Cp*, pentamethylcyclopentadienyl(1−); Et_2dtp, *O,O'*-diethyl dithiophosphate(1−); $HB(Me_2pz)_3$, hydrotris(3,5-dimethylpyrazolyl)borate(1−); L-NS_2, 2,6-bis(2,2-diphenyl-2-sulfidoethyl)pyridine(2−); pip, piperidyl; pyO, pyridine *N*-oxide; R_2dtc, N,N-disubstituted dithiocarbamate(1−); sap, 2-(salicylideneamino)phenolate(2−); solv, solvent ligand; ssp, 2-(salicylideneamino)benzenethiolate(2−).
(18) Topich, J.; Lyon, J. T., III. *Polyhedron* **1984**, *3*, 55, 61.
(19) Topich, J.; Lyon, J. T., III. *Inorg. Chem.* **1984**, *23*, 3202.

0020-1669/89/1328-4385$01.50/0